Microfluid Nanofluid (2015) 18:739–753
DOI 10.1007/s10404-014-1510-z

REVIEW

The applications of pressure-sensitive paint in microfluidic systems

Chih-Yung Huang · Yu Matsuda · James W. Gregory · Hiroki Nagai · Keisuke Asai

Received: 28 April 2014 / Accepted: 27 October 2014 / Published online: 11 November 2014

Abstract Pressure-sensitive paint is an experimental technique that has been developed for decades and recently applied for microscale measurements to retrieve surface pressure data. Promising results have been reported at various flow regions including transition flow, supersonic flow, and unsteady flow regimes. The experimental results acquired by pressure-sensitive paint have been compared with computational simulation and theoretical analysis, and good agreements have been established. This technique provides not only qualitative information but also quantitative data for the flow field inside microfluidic systems. This paper summarizes the methodology and applications of pressure-sensitive paint in microscale measurements as well as their usage for oxygen detection in several areas. Critical comments and future aspects of the technique have also been provided.

Keywords Pressure-sensitive paint · Microfluidics · Experimental measurement · Pressure · Internal flow field

C.-Y. Huang (✉)
Department of Power Mechanical Engineering,
National Tsing Hua University, Hsinchu 30013, Taiwan
e-mail: cyhuang@pme.nthu.edu.tw

Y. Matsuda
Department of Micro-Nano Systems Engineering,
Nagoya University, Nagoya, Japan

J. W. Gregory
Department of Mechanical and Aerospace Engineering,
The Ohio State University, Columbus, OH 43235, USA

H. Nagai · K. Asai
Department of Aerospace Engineering, Tohoku University,
Sendai, Japan

1 Introduction

Microfluidic systems have been used and studied extensively in the twenty-first century. With emerging applications, there has been significant interest in studying the physics in such small-scale dimensions, from millimeter to micrometer, or even sub-micrometer. Physical phenomena at microscale differ from those in macroscale. At microscale, viscous effects and compressibility effects are more apparent. Slip boundary conditions and rarified gas effects are encountered. These phenomena can also be characterized by the changing in values of analyzed dimension and dimensionless numbers: The characteristic length decreases, the Knudsen (Kn) number increases, and Reynolds (Re) number decreases. For example, when the characteristic length of a microfluidic device becomes smaller and closer to the mean free path of fluid molecules, the fluid regime changes from continuum regime to transition regime, and even to free-molecule flow regime. At free-molecule flow regime, the fluid molecules do not move one after another as in the continuum flow. Instead, the molecule behaves like particle, due to the large spaces between each molecule. The Re number in the microfluidic flow field is relatively small compared with that in macroscale systems; in other words, the influence of viscous forces becomes comparable to that of inertial forces. Rapidly growing viscous layers inside microfluidic devices due to low Re numbers are observed in several reports (Alexeenko et al. 2000; Buoni et al. 2001; Ivanov et al. 1999). The dislike physical phenomena between macro- and microscale systems need to be investigated thoroughly to improve the performance of various microfluidic devices (Ho and Tai 1996, 1998; Karniadakis and Beskok 2002; Nguyen and Wereley 2002). Although microparticle image velocimetry (micro-PIV) and laser-induced fluorescence

(LIF) have been proven to provide decent results for liquid flow (Chamarthy et al. 2010; King et al. 2007; Meinhart et al. 1999a, b), most of the existing research for illustrating internal flow/temperature field of gas is limited to simulation and theoretical analysis. For example, simulations with DSMC (Direct Simulation Monte Carlo) and Navier–Stokes approaches have been used for analyzing flow fields in micronozzles and microchannels (Alexeenko et al. 2000; Beskok et al. 1996). Additionally, micro-PIV only provides the flow field without revealing the pressure difference inside the device. Other than micro-PIV, only few experimental techniques have been utilized for studying the internal flow in microfluidics due to the difficulty in embedding sensors (Beskok 2001; Beskok et al. 1996; Jie et al. 2000; Roy et al. 2003). Therefore, the experimental investigations in microfluidics are restricted to the measurements of the external flow field. Miniature pressure transducers with the size of a few hundred micrometers were installed in microchannel devices, but only discrete data points can be acquired and the spatial resolution of experimental data is limited to a couple hundred micrometers due to the size of pressure sensors (Agrawal 2011; Hong et al. 2012; Morini et al. 2011; Pong et al. 1994; Tang et al. 2007; Wereley and Jang 2004; Zohar et al. 2002).

The experimental method utilizing molecule-based pressure sensors, also known as pressure-sensitive paint (PSP), has been developed in 1980s (Liu and Sullivan 2004). PSP technique uses a non-intrusive optical approach to acquire the pressure data on the model surface through luminescence signal emitted from the pressure-sensitive molecule. It offers not only qualitative information such as high-quality flow visualization profile, but also quantitative pressure data. PSP technique has the advantages of simple and fast preparation, and it is capable of acquiring global pressure profiles with high spatial resolution as fine as a few micrometers. These characteristics make it an excellent experimental technique for pressure measurements at the macroscale, such as measurement of aerodynamic forces in wind tunnel or flight tests. Inspired by the success of PSP measurements at macroscale, researchers have extended the application of PSP technique to microscale flow measurements. The flow fields inside microdevices have been successfully measured by Huang et al. (2002), where they reported the pressure distribution inside a micronozzle device. Subsequent research applying PSP sensors in various microdevices has been conducted with microchannel, micronozzle, microcone, microjet, microturbine, and microfluidic oscillator devices (Gregory et al. 2007; Guo et al. 2008; Huang 2006; Huang et al. 2006, 2007a, b; 2008, 2012; Huang and Lai 2012; Nagai et al. 2008; Osafune et al. 2004). The comparison between PSP and other experimental methods applied on pressure measurements in microchannel flow is listed in Table 1. It is

Table 1 Comparison of pressure-sensitive paint and other experiment methods in microchannel flow

Experimental method	Pressure-sensitive paint	Optofluidic membrane interferometer	Micromembrane pressure sensor	Conventional pressure transducer
Pressure range	0–0.2 MPa	0–10 psi	0.1–0.4 MPa	0–1 MPa
Typical uncertainty	3 %	±2 %	3–5 %	0.25 %
Internal/external measurement	Internal	Internal	Internal	External
Measurement type	Noninvasive (optical access to luminescence signal)	Noninvasive (optical access to interference from air-gap cavity)	Invasive (pressure measurement through pressure taps connected to the main channel)	Invasive (pressure measurement through pressure taps connected at inlet and exit plenum)
Sensor size	A couple nanometer	~200 × 480 μm^2	100 × 100 μm^2	6–60 mm
Spatial resolution	1.6–3 μm per data point	530 μm (the air-gap cavity positioned at inlet and exit of microchannel)	~650 μm per data point	28–100 mm (transducers positioned at microchannel inlet and exit)
Working fluid	Air and oxygen	Liquids	Gases (Helium, Argon, Nitrogen)	Gases and liquids
References	Huang and Lai (2012), Matsuda et al. (2011c)	Song and Psaltis (2011)	Zohar et al. (2002)	Tang et al. (2007)

noticed that conventional pressure transducer has better accuracy (0.25 %) compared with PSP technique (3 %). The poor accuracy of PSP measurement is attributed to the low signal-to-noise ratio, which is resulted by the thin paint layer at microscale, i.e., low luminescence. However, PSP technique can provide pressure data with superior spatial resolution (3 μm) compared with hundred micrometers of micromembrane pressure sensor and several millimeters for pressure transducer. In microchannel measurements, the spatial resolution of conventional pressure transducer is often in the order of millimeter to centimeter, which is the length of microchannel, because the transducers are positioning at inlet and outlet of microchannel. Although efforts have been made for using conventional transducers to measure the pressure inside microchannel through pressure taps and small pockets next to the channel, the quality of acquired experimental data is similar to those using micromembrane pressure sensor (Hong et al. 2012; Wereley and Jang 2004). The great spatial resolution of PSP measurements provides pressure evolution with great detail in the region of interest for studying gas behavior in microscale. In addition, PSP technique also provides two-dimensional pressure map, which can help understand asymmetric flow field in the region with aggressive change in geometry. Microfluidic investigations from classic microchannel flow to unsteady flow in a microfluidic oscillator have also been performed using PSP technique. The detailed pressure profiles acquired by PSP sensors provide essential information for studying the physics at microscale. In this paper, the comprehensive methodology of PSP technique is discussed and recent works utilizing this technique in various microfluidic devices are summarized.

2 Principle of PSP measurement

PSP technique has been applied in aerospace engineering since 1980s. The technique uses molecule-based sensors consisted of luminescent molecules and binder. During the measurement, the intensity variation of luminescent molecules (luminophore) is recorded, calibrated, and then translated into pressure data. Figure 1 presents the schematic of PSP measurement. A binder can be polymer or porous substrate on model surface. It is used to attach PSP sensors on the model surface and helps the sensors to survive during various test conditions as harsh as supersonic flow. PSP sensors are irradiated with excitation light source at specific wavelength during the experiment. A UV, blue, or green LED lamp, depending on the selected luminescent molecules, can be used to excite the luminescent molecules. The energy level of PSP molecule is raised to high energy state during excitation, and it returns to ground state through either radiative process or non-radiative

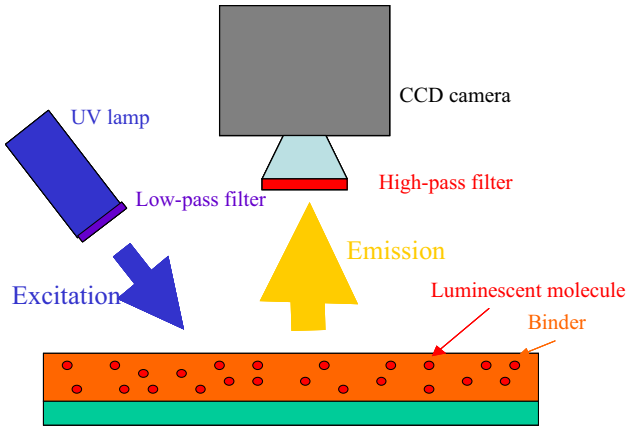

Fig. 1 Schematic of PSP measurement ©[2007]IEEE. Reprinted with permission from (Huang et al. 2007b)

process. The radiative process emits luminescence with longer wavelength than the excitation wavelength, and this phenomenon is known as stokes shift. The difference in excitation and emission wavelengths makes it straightforward to collect only emission light if suitable optical filter is applied. The experiments are generally carried out in a dark room or at night, use optical filters to remove the light from environment, and improve the signal-to-noise ratio. The non-radiative process for PSP measurement is oxygen quenching which is the result of interaction between oxygen molecules and luminophores. Oxygen quenching will reduce the energy available to the radiative process, i.e., the higher the oxygen concentration, the lower the luminescence. Therefore, the luminescence changes with the variation of oxygen concentration in the environment. Based on Delton's and Henry's law, the detected oxygen concentration from luminophore in the binder can be further calibrated as the measured static pressure under the assumption of a fixed proportion of oxygen molecules in the air. The Stern–Volmer equation can be used to calibrate pressure and luminescence variation:

$$\frac{I_{\text{ref}}}{I} = A(T) + B(T)\frac{P}{P_{\text{ref}}} \tag{1}$$

Here, I is the luminescence acquired during the test, and I_{ref} is the luminescence measured at a reference condition, while A and B are temperature-dependent coefficients to be obtained via calibration. After obtaining A and B, the Stern–Volmer equation can be applied to translate the luminescence intensity to the pressure data at an unknown condition. More details of PSP measurement at macroscale can be found in the reference from Liu and Sullivan (2004).

In order to apply PSP sensors inside microdevices, a coating procedure, which can precisely control the paint thickness, has been developed to replace conventional compressed air-spraying processes in macroscale

measurements. The spin-coating method, adapted from standard MEMS fabrication processes, is used to apply PSP sensor coating on a glass slide, creating a thin and uniform layer with about 1 μm thickness and 0.06 μm surface roughness (Huang et al. 2007b). The glass slide with PSP sensor will be used as cover glass to seal microfluidic devices. The spin-coating method provides a simple and easy way to apply PSP sensors for microscale measurements. The size of the luminescent molecules selected for PSP sensor is of the order about 1 nm and can be embedded inside the microdevices with massive numbers. Studies of other PSP coating methods have been carried out by Matsuda et al. (2007, 2009b), Sakamura et al. (2014) to improve fabrication processes in preparing PSP sensors for micro- or nanoscale measurements. They reported the Langmuir–Blodgett method to prepare pressure-sensitive molecular films (PSMF) with an amphiphilic luminophore (Matsuda et al. 2011c). Matsuda et al. (2011a) also proposed another method for fabricating microchannels with PDMS containing luminophore (pressure-sensitive channel chip, PSCC) to enhance luminescent signal in microscale measurements. The feasibility of using PSMF and PSCC has been demonstrated, and they provide alternative options for PSP sensor preparation in micro- and nanoscale research. The spin-coating process can be used to prepare PSP sensors with sensor thickness around micrometers, while the Langmuir–Blodgett method should be used if the sensor thickness of a couple monolayers is needed. These two coating methods provide the precise control of sensor thickness at micro- and nanoscale, while the conventional compressed air-spraying method results in paint thickness around hundreds of micrometers. The luminescence intensity in microscale measurements was considerably lower compared with that in macroscale measurements, and this is the consequence of thinner layer of PSP sensor, i.e., less embedded luminophores. The sensor thickness also has impact on the procedure of data reduction for PSP sensor, while the assumption of one-dimensional oxygen permeation is applied, and the influence will be discussed in the following section.

During the macroscale measurement, a photodetector (a photomultiplier tube, PMT, or a CCD camera) is used to collect the luminescence variation. A long-pass filter is installed in front of the photodetector, and a short-pass filter is installed on the excitation light source to separate the excitation and emission signals, as well as to eliminate the noise coming from the environment. Before the measurement, a reference image is recorded at reference condition. Generally, the reference image is taken at ambient pressure. The reference image provides intensity profile for normalizing data obtained during experiments (Liu and Sullivan 2004). The normalized intensity ratio is used for calculating the pressure data using the calibration (for example, Stern–Volmer equation) which can be completed before or after the experiment. Other than intensity-based measurements, lifetime decay method has been utilized to solve issues of temperature dependence and demanding reference images (Crafton et al. 2005; Goss et al. 2005; Peng et al. 2010). However, two integration periods (gate) are needed during data acquisition with an integration time of around 10 ns (Crafton et al. 2005; Goss et al. 2005; Mitsuo et al. 2006). Due to the thin sensor coating thickness (~1 μm) in microscale measurements, low luminescence intensity observed from the experiments poses barriers to the application of lifetime decay method.

There are several PSP sensors that have been applied in microfluidic research, and they are summarized in Table 2. These PSP sensors are effective at pressure ranges from 200 Pa to 400 kPa or higher (Liu and Sullivan 2004). With careful selection of the binder and luminescent molecules, PSP sensor is also capable of acquiring unsteady flow fields (Gregory et al. 2014). One of the important advantages of PSP sensor in gas phase microfluidic research is the great pressure sensitivity at near-vacuum condition, which falls in the region having the deeper slope on the calibration curve shown in Fig. 2. The great pressure sensitivity at low pressure region can provide excellent pressure resolution during the microscale measurements. This advantage can be utilized by microfluidic researchers pursuing flow phenomena at high-Kn number situation (transition or free-molecular regimes). However, further investigations regarding molecular behavior at free-molecular regime are required before this technique can be applied to practical measurements. To date, most applications of PSP sensors in microfluidic systems are still limited to the micrometer scale and transition regime (Kn below 0.4). In these regimes, Delton's law, which claims that the proportion of oxygen molecules is fixed and homogeneous in the air, allows the oxygen concentration to be calibrated as static pressure. However, while the scale is down to micrometer or even nanometer, molecule dynamics is required instead of continuum assumption to describe the fluid behavior. The different molecular weights between oxygen and nitrogen molecules will cause dissimilar movements, and the assumption of uniform distribution of molecule is no longer valid. In this case, detailed investigation of molecule movement must be performed, or specific statement of oxygen concentration must be included while translating the luminescence signal from an oxygen-sensitive PSP sensor. Applications of PSP on micro- or nanometer scale measurements have been investigated by Matsuda et al. with PSMF sensors (Matsuda et al. 2007, 2009a, b). However, the translation of intensity readings to static pressure instead of oxygen concentration at the sub-micrometer scale (free-molecular flow regime) still needs to be established. Efforts have been made in discussing the appropriate situation using PSP sensor to measure

Table 2 PSP/TSP applications in microfluidics

PSP/TSP sensor	Binder	Pressure/temperature measurement	Microfluidic device
Pt(II)meso-Tetra(Pentafluorophenyl) Porphine (PtTFPP)	TMSP (1-trimethysilypropyne)	Pressure	Microchannel, Micronozzle, Microturbine (Huang et al. 2006, 2007a, b)
Pd(II)meso-Tetra(Pentafluorophenyl) Porphine (PdTFPP)	TMSP (1-Trimethysilypropyne)	Pressure	Microchannel (Huang et al. 2007b)
Pt(II)meso-Tetra(Pentafluorophenyl) Porphine (PtTFPP)	PDMS (Polydimethylsiloxane)	Pressure	Microchannel (Huang and Lai 2012; Matsuda et al. 2011a)
Pt(II)meso-Tetra(Pentafluorophenyl) Porphine (PtTFPP)	Poly TMSP (poly(1-Trimethysilypropyne))	Pressure	Microturbine (Huang et al. 2006)
Pt(II)meso-Tetra(Pentafluorophenyl) Porphine (PtTFPP)	Poly(IBM-co TFEM)	Pressure	Micronozzle (Nagai et al. 2008), Microcone (Osafune et al. 2004)
Tris (Bathophenanthroline) ruthenium dichloride	Anodized aluminum	Pressure	Microfluidic oscillator (Gregory et al. 2005)
Bathophen Ruthenium Chloride	GE RTV 615	Pressure	Micronozzle (Huang et al. 2002)
Pt(II) Mesoporphyrin IX (PtMP)	Pressure-sensitive molecular film (PSMF)	Pressure	Micronozzle (Matsuda et al. 2011c)

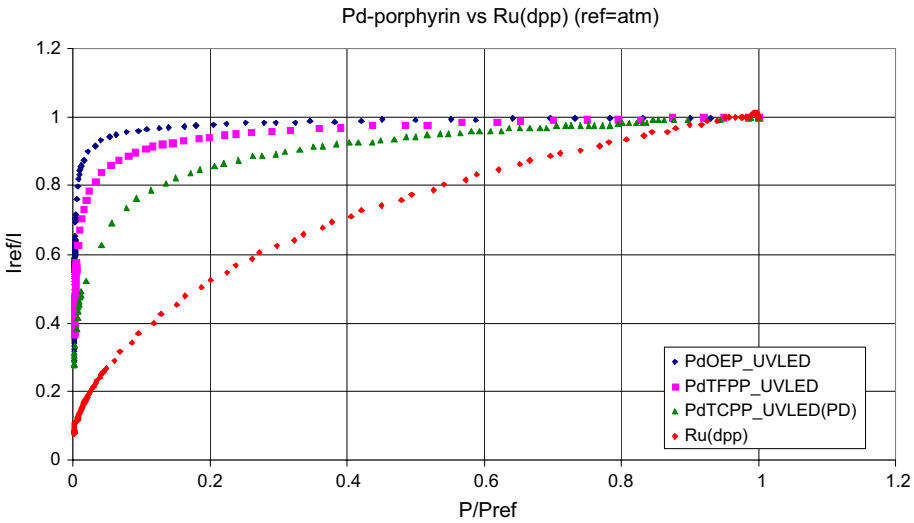

Fig. 2 Calibration curves of PSP sensors of Pd-Porphyrin and Ru(dpp) (Huang 2006)

either thermodynamic pressure or surface pressure only. The PSP sensor at micro- or nanoscale will be better treated as "molecular number flux sensor" (Yamaguchi et al. 2009). More detailed investigation or experimental validations are still needed for this not fully identified application regime.

3 Measuring method

The apparatus for PSP experiments in microscale includes an excitation light source, a photodetector, selected optical filters, and PSP sensors, similar to the conventional measurements in macroscale. A photodetector is used to collect the luminescence emitted from PSP sensors during excitation. The optical filters generally include one short-pass filter and one long-pass filter. The short-pass filter is positioned in front of excitation light source to ensure the precise and clean excitation wavelength. The long-pass filter is positioned in front of the photodetector, to remove background noise in the luminescence. However, in order to magnify the image and improve the spatial resolution of PSP measurements at microscale, several approaches can

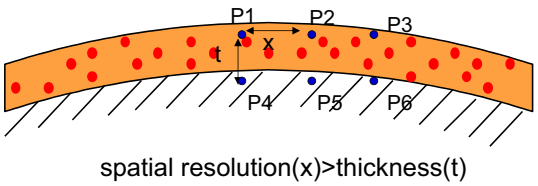

Fig. 3 One-dimension assumption of PSP/TSP measurement (Huang 2006)

be applied. The spatial resolution from PSP measurement mainly depends on the photodetector, where it can be a single-point measurement (with a photomultiplier tube, PMT) or a two-dimensional measurement (with a CCD camera). An increase in the pixel resolution on the CCD chip will improve the resolution of global pressure map; this resolution will continue to improve as CCD technology evolves. The other way to increase the spatial resolution is the use of an optical arrangement involving camera bellows, a close-up lens, or a microscope. For the applications in microscale measurements, a florescence microscope can be adapted with a highly sensitive CCD camera to capture the luminescence profile inside microfluidic devices. The excitation and emission signals can be separated by optical filters and a dichroic mirror that are accessible for most fluorescence microscope. With the help of microscope, the spatial resolution of PSP measurement has been enhanced to sub-micrometer. However, one should cautiously uses the one-dimensional oxygen permeation assumptions during data reduction. One-dimensional oxygen permeation assumption is only valid when the thickness of paint layer is smaller than the dimension of diffraction pattern caused by oxygen diffusion. In other words, the spatial resolution is bound to be lower than the paint thickness, which is around sub-micrometer when spin coating is applied. One-dimensional oxygen permeation assumption is generally applicable for macroscale measurements, in which the paint thickness is around hundreds of micrometers and the spatial resolution in the pressure map is in the scale of millimeter. However, the coating thickness of PSP sensor in the microscale measurement is around a few micrometers, and the spatial resolution in the magnified images under microscope is close to or less than the paint thickness. Therefore, this assumption is doubtful and needs to be re-examined or corrected. Figure 3 presents the schematic of one-dimensional oxygen permeation assumption. During PSP measurements, the acquired luminescence from location P2 should include only the emission from sensors at P2 and sensors underneath it (P5) if the thickness t is smaller than the pixel distance x. However, if the thickness is greater than the pixel distance, the luminescence acquired at location P2 will be contributed not only by P2 and P5, but also by nearby locations, for example, P4 and P6 due to comparable distance between P2–P5 and P2–P4/P6. Therefore, the pressure profiles acquired by PSP measurements will be compromised and smeared if without proper correction using equation of two-dimensional oxygen permeation/diffusion process. Recent studies have reported that a resolution about 8.5 times of the thickness of PSP sensor can be achieved when measuring continuous variation of pressure. For a pressure jump such as a shock wave, the spatial resolution is about 5 times of the thickness of a PSP layer (Matsuda et al. 2012; Mosharov et al. 1997).

Another challenge that has been reported during microscale measurements is the inconsistent calibration behavior from pixel to pixel in the intensity map. In macroscale measurement, the normalization procedure is performed to eliminate the effects from non-uniform paint thickness and excitation light. However, this typical normalization procedure is not sufficient to correct the discrepancy observed in the microscale measurements. Due to the reduced thickness, the paint layer is partly transparent and this makes the detection sensible to the surrounding noises. Therefore, pixel-by-pixel calibration in the microscale measurement, especially at a scale of around 100 μm, is suggested for removal of surrounding noises. The pixel-by-pixel calibration is carried out by treating each individual pixel on the CCD chip as an individual pressure probe and applying individual calibration equation for each pixel. In conventional PSP measurements, every pixel in the image is calibrated by the same calibration equation. The pixel-by-pixel calibration resolved up to 77 % error due to discrepancy from calibration curves (Huang et al. 2012). However, it lengthened the computation time for data reduction, depending on the number of pixels on the CCD sensor. In summary, the principle of PSP measurement and main components in the experimental apparatus, including excitation light source, photodetector, and selection of optical filters, are similar in macro- and microscale applications. The major differences between PSP technique in macro- and microscale measurements are the integration of microscope in the microscale measurements, additional correction method such as pixel-by-pixel calibration to adapt to the constrains in microscale measurements, and preparation of thin PSP paint layer in microscale measurement using spin-coating or Langmuir–Blodgett method instead of air spray. The similar apparatus makes it easier for researchers to conduct microscale PSP measurements if they already have experience and hardware from the macroscale measurements.

4 The applications of PSP sensors in microfluidic systems

The experimental results acquired by PSP sensors are presented in the following sections in the categories of: (1)

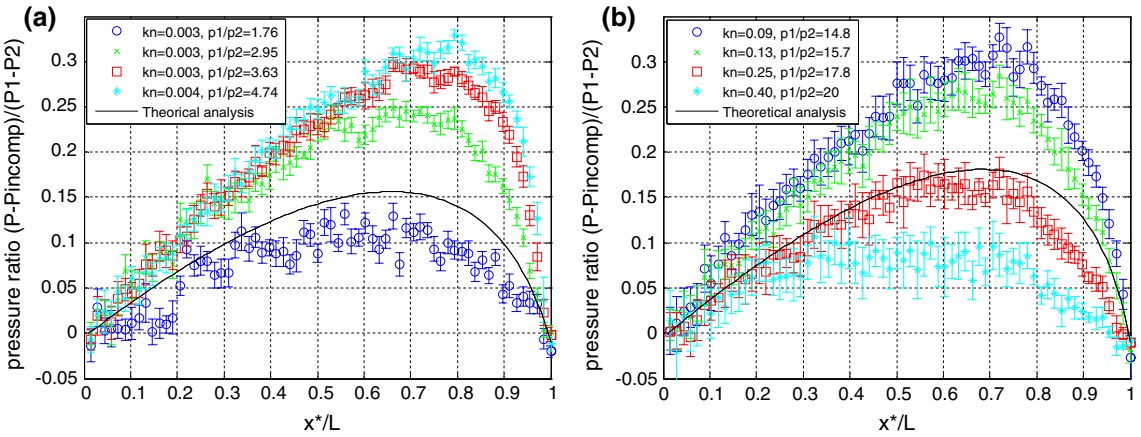

Fig. 4 **a** Pressure distribution along the centerline in a microchannel with different P_{in} and P_{exit} ratios, **b** pressure distribution along the centerline in a microchannel with different Kn numbers. ©[2007]IEEE. Reprinted with permission from (Huang et al. 2007b)

continuum to transition flow regime measurements, (2) supersonic flow measurements, (3) unsteady flow measurements, and (4) oxygen detection in microfluidic devices. Examples of pressure profiles obtained by PSP measurements inside or outside the microfluidic devices with detailed pressure data in different flow conditions are also included.

4.1 PSP measurements in continuum and transition flow regimes

The PSP sensor, Pd(II)meso-Tetra(Pentafluorophenyl) Porphine (PdTFPP), has been demonstrated with high sensitivity from near vacuum to 14 kPa, which can be seen from the calibration curve of PdTFPP in Fig. 2, making it feasible to investigate pressure distribution inside microchannel for flow regimes from continuum to transition flow where Kn varies from 0.003 to 0.4. The pressure distributions acquired by PSP sensors not only provide the pressure map inside the channel but also have sufficient spatial resolution at the channel entrance for observing the pressure drop due to the entrance effect.

4.1.1 Pressure measurements in straight microchannels

The flow inside the straight microchannel with rectangular cross section has been investigated with PSP sensors of Pt(II)meso-Tetra(Pentafluorophenyl) Porphine (PtTFPP) and PdTFPP. A 12.5-mm-long, 235-μm-wide, and 112-μm-deep rectangular channel is connected with two pressure chambers at entrance and exit to control and maintain the pressure inside the channel. The pressure distribution acquired by the PSP sensor shows compressibility effects: The nonlinearity of pressure distribution increases as the pressure ratio between the inlet and exit increases. The rarefaction effect is also observed with the flattening of the pressure distribution inside the microchannel, while Knudsen number increases from 0.09 to 0.4 (continuum to transition flow regime). The results are shown in Fig. 4a, b, in which the pressure distribution is recorded along the centerline of the microchannel. The pressure map at the channel entrance and the normalized pressure at the center are shown in Fig. 5 (Huang et al. 2007b). The high spatial resolution provides sufficient experimental data to study the pressure drop at entrance, and the data show good agreements with simulation results obtained by Guo et al. (2008), which use a Navier–Stokes solver with slip and no-slip boundary conditions to investigate differences of the gas flow in 2D and 3D microchannels.

4.1.2 Pressure measurements in constricted microchannels

Recent applications of PSP in the microchannel flow have been further extended to constricted microchannel flow (in continuum flow regime), and 3 μm per data resolution has been realized in the pressure profiles after applying pixel-by-pixel calibration (Huang and Lai 2012; Huang et al. 2012). Taking the advantages of two-dimensional pressure map acquired by PSP technique, the flow pattern after sudden constriction can be investigated with detail. Figure 6 presents the pressure maps inside constricted microchannel with aspect ratio of 1.49:1 (channel width/channel depth) and constricted ratio of 1:2 (rib height/channel width) at different Reynolds numbers and the enlarged pressure contour near the constriction (Huang and Lai 2012). Axisymmetric pressure distributions upstream from constricted ribs are founded in the pressure maps, as well as the region after the ribs. Asymmetrical pressure distribution due to flow deflection after

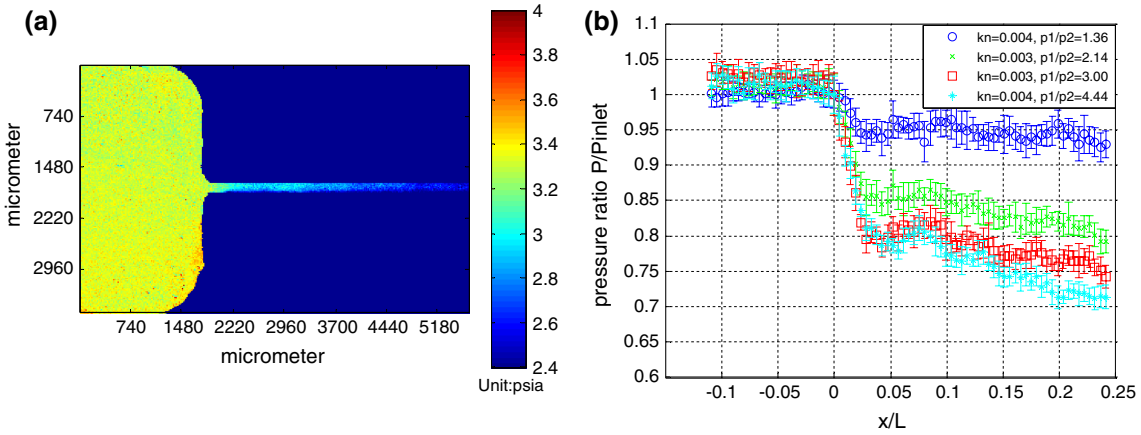

Fig. 5 **a** Pressure map acquired at channel entrance, **b** pressure distribution along the centerline at channel entrance with different pressure ratios. ©[2007]IEEE. Reprinted with permission from (Huang et al. 2007b)

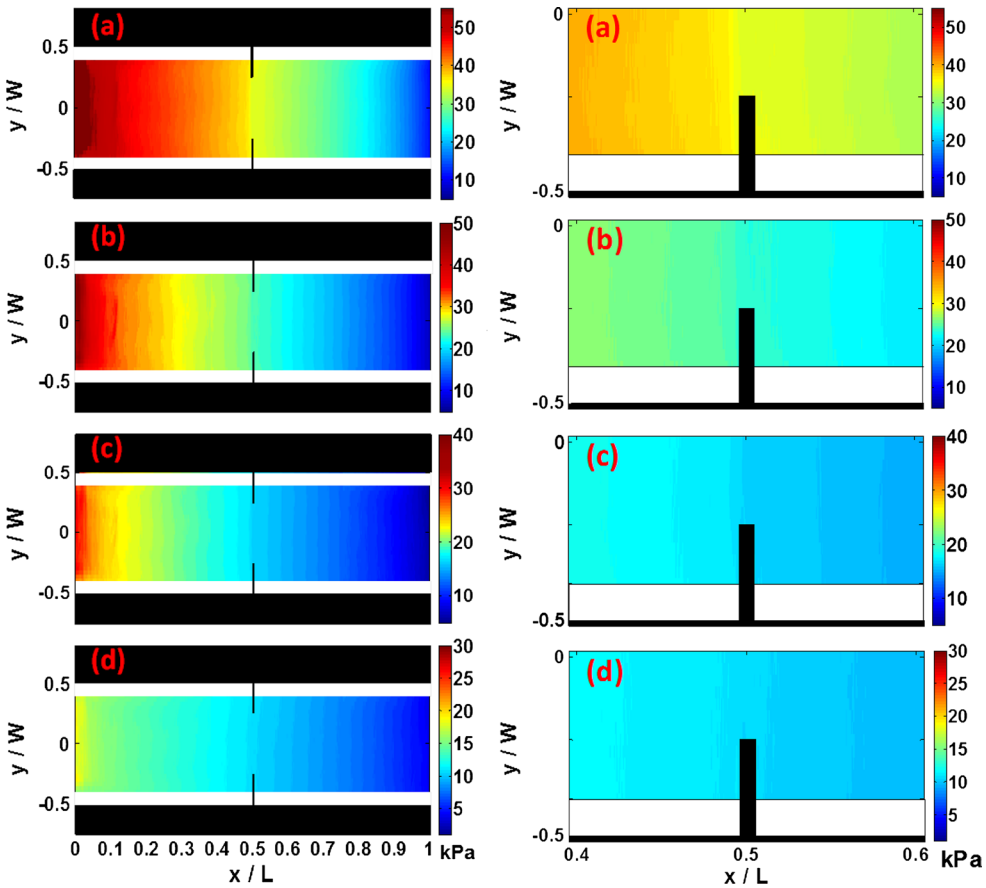

Fig. 6 *Left* The pressure maps of a constricted microchannel acquired by PSP at **a** Re was 78, **b** Re was 50, **c** Re was 27, and **d** Re was 9. *Right* The enlarged pressure maps around the constriction region at **a** Re was 78, **b** Re was 50, **c** Re was 27, and **d** Re was 9. Figure adapted with permission from IOP Publishing (Huang and Lai 2012)

constriction structure has been confirmed with various constricted microchannels having higher aspect ratio (1:1) and constricted ratio (4:5) (Chiang et al. 2013). These results demonstrate the capability of PSP technique in presenting two-dimensional pressure profiles for microfluidic research.

4.1.3 Molecular flux measurement in rarefied gas flow

The application of PSP technique on rarefied gas flow has been attempted with 0.5-mm jet impingement in the controlled region where pressure is blow 130 Pa, which has a high-Kn number of 22.4. The luminescence signal from

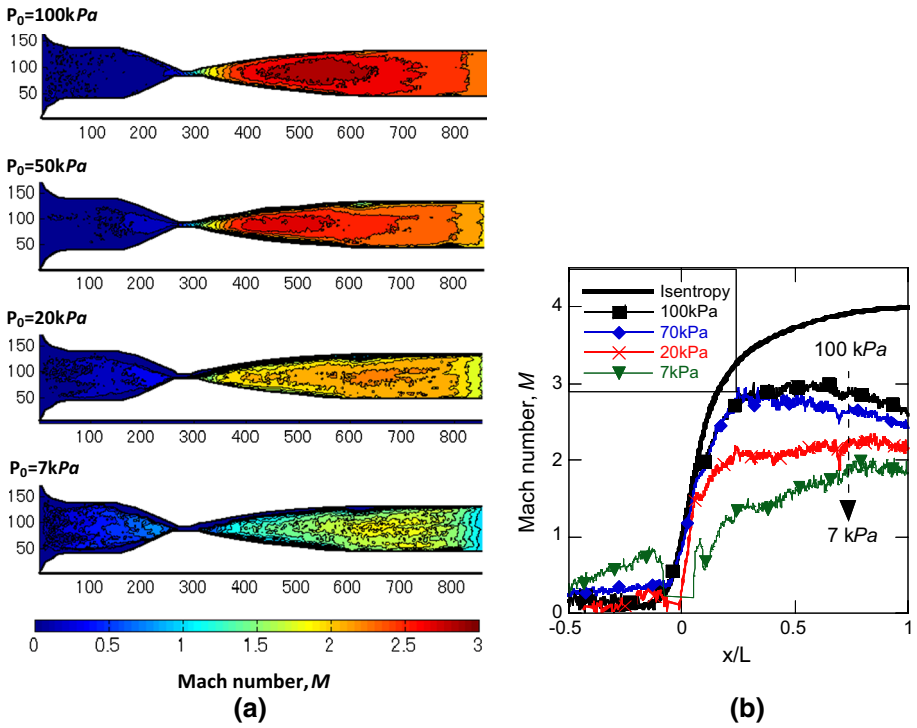

Fig. 7 **a** Pressure map inside micronozzles at different test conditions, **b** the comparison of Mach number calculated from isentropic analysis and experimental data. Figure adapted from Nagai et al (2008) with permission of the American Institute of Aeronautics and Astronautics, Inc. (Nagai et al. 2008)

PSP during the experiment has been further examined while determining the translation to pressure or oxygen pressure for high-Kn number flow. The molecular number flux has been considered as the information presented by PSP measurement, which is important for analyzing the interaction of flow and solid surface if Kn number greater than one (Mori et al. 2005). Yamaguchi et al. (2009) reported that experimental data acquired by PSP measurements agreed with the DSMC results calculating the normal stress introduced by incident gas molecules to the surface, which is equivalent to the change in the normal momentum flux to and from the surface, not the thermodynamic pressure. The result reveals the capability of PSP measurement for high-Kn flow; however, this is a new area of PSP technique and more efforts are needed for further applications.

4.2 PSP applications in supersonic flow measurements

The qualitative and quantitative data acquired by PSP sensors have been used to locate the shock wave in a supersonic flow field inside the micronozzle. A rapidly growing viscous boundary is observed in the divergent section in the nozzle, and it expedites flow transition from supersonic to subsonic.

4.2.1 Pressure measurements in supersonic micronozzles

The pressure distribution in a De Laval type micronozzle with the throat height of 250 μm has been acquired using PSP sensor PtTFPP. Shock wave structure is observed as the pressure drops dramatically in the divergent section under the condition of inlet pressure of 380 kPa (55 psi), and pressure ratio between inlet and exit is 3.86. The strength of the shock waves dissipates, and the boundary layer grows rapidly while the inlet pressure decreases (Huang et al. 2007a). Experimental results from Nagai et al. (2008) also show the Mach contour of supersonic flow in a micronozzle. The Mach number profiles along the centerline of the nozzle are shown in Fig. 7a, which validates that the Mach number distribution in a microfluidic device such as the micronozzle can be captured by PSP sensors. A similar trend can be observed in these studies: The Mach number in the downstream region decreases, and the boundary layer grows as the total pressure decreases. The increasing deviation between the experimental results and the isentropic flow analysis is shown in Fig. 7b. The effect of the viscosity increases because the Re number decreases with decreasing total pressure, and consequently, the influence of the boundary layer on the flow becomes stronger.

The pressure distribution in a micronozzle obtained by PSMF is reported by Matsuda et al. as shown in Fig. 8 (Matsuda et al. 2011c). The micronozzle has a 2D converging–diverging geometry with the throat width of 103 μm, diverging length of 492 μm, and diverging angle of 23.5°. The depth of the nozzle is 1.0 mm. A slide glass with PSMF is put on the nozzle as a cover. The luminescence from PSMF is collected by a fluorescence microscope and an EM-CCD camera. Using an objective lens with 10

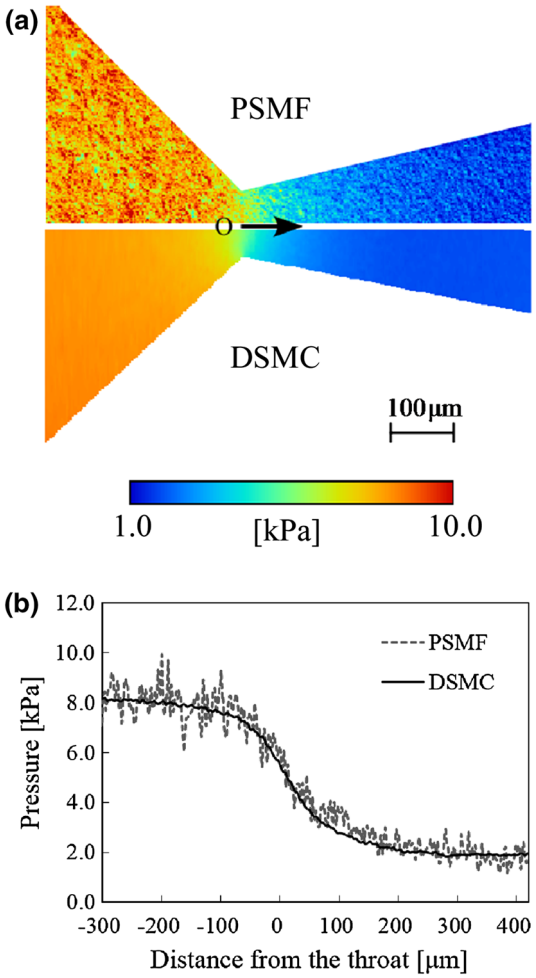

Fig. 8 Pressure distribution in a micronozzle measured by PSMF. Figure adapted from Matsuda et al (2011c) with kind permission from Springer Science and Business Media. (Matsuda et al. 2011c)

times magnification, the spatial resolution is 1.6 μm per pixel. The inlet and outlet pressures are 10.0 and 1.0 kPa, respectively. Figure 8a shows the pressure distribution in the micronozzle. The pressures along the centerline of the nozzle and the numerical simulation by DSMC are plotted in Fig. 8b, showing that the pressure distribution obtained by PSMF agrees very well with that by DSMC. Another attempt of PSP measurement in a supersonic nozzle with size of 9.6 mm has been carried out by Zare-Behtash et al. The shock cell has been successfully identified from the pressure maps acquired by PSP technique, and the results agree with the flow visualization images obtained using Schlieren technique (Zare-Behtash et al. 2009).

4.2.2 Pressure measurements with a supersonic cone

Osafune et al. (2004) applied PSP sensors on a 2-mm-diameter cone–cylinder model and demonstrated the surface measurement for microscale objects by PSP sensors. Figure 9a shows the surface pressure distribution on the cone at Mach number 1.89. The surface pressure on the cone is mostly uniform except for that on the tip region. The pressure difference between cone and cylinder is also visualized distinctly. Figure 9b shows the good agreement between pressure profiles obtained by PSP and the computational fluid dynamics (Reynolds-averaged Navier–Stokes equation, RANS) except for the region around nose. As stated in Sect. 4.1.3, the agreement will be improved significantly in the nose region, if the normal stress, not the thermodynamic pressure, calculated by DSMC is compared with the PSP measurement.

4.2.3 Pressure measurements of supersonic microjet impingement

Another example of applying PSP sensors on supersonic flow field is supersonic microjet impingement. Due to the small characteristic length in the microscale flow field, the Re number is small and the viscous effect starts to dominate the flow field. Flow velocity after exiting the microjet decreases rapidly, and the most flow impingement is subsonic; therefore, not much work has been found for supersonic microjet impingement using jet size of micrometer. Figure 10 shows the pressure map of a 1-mm microjet impinging at an angle of 10 degree with respect to the surface. The shock wave pattern is clearly shown in the

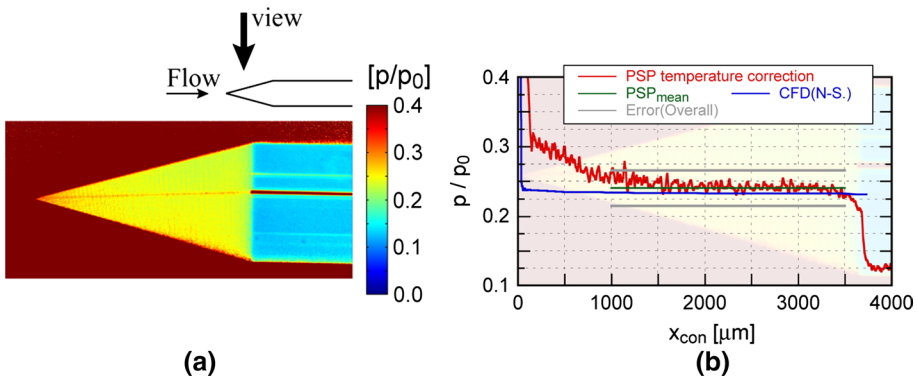

Fig. 9 **a** Surface pressure distribution on the cone at Mach number 1.89, **b** the comparison of simulation and experimental data. Figure adapted from Osafune et al. (2004), courtesy of Prof. Keisuke Asai. (Osafune et al. 2004)

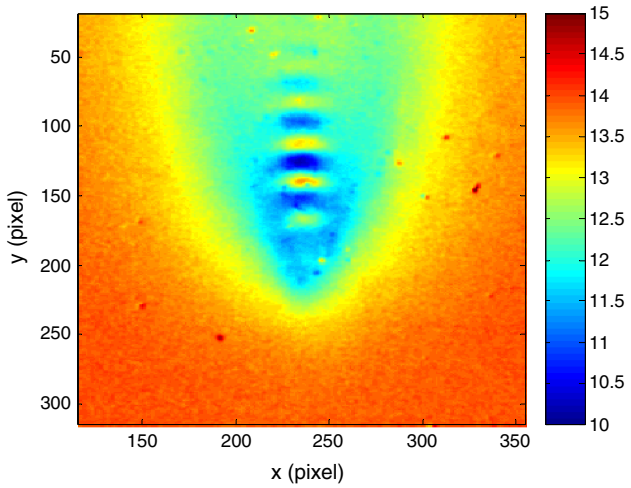

Fig. 10 Pressure map of a 1-mm microjet impinging at the angle of 10° with respect to the surface (Huang et al. 2008)

pressure data, as is the pressure jump in the downstream of the jet exit (Huang et al. 2008). Another study of supersonic microjet impingement has been done by Crafton et al., using larger nozzle of 5 mm and two impinging angles of 10 and 20 degree (Crafton et al. 1999). With larger nozzle size, the shock wave patterns captured by PSP measurement are clear to see with stronger strength and higher pressure fluctuation. The locations of maximum pressure recovery are also analyzed, and they are found upstream from the geometric impingement point and independent of Re number.

4.3 PSP applications in unsteady flow

One of the most challenging experiments in microfluidic devices is measuring unsteady flows. The challenges involve not only the small size of microfluidic devices but also the requirement of fast response from the sensor.

4.3.1 PSP measurements in a microfluidic oscillator

In order to demonstrate that the PSP sensor is capable of unsteady flow measurement, a microfluidic oscillator was used to investigate frequency response (Gregory et al. 2007). Pressure variation was acquired at a frequency of 9.4 kHz, which was near the low end of the frequency range of the device, at a relatively low flow rate (550 mL/min or ~0.67 g/min, with a supply pressure of 6.69 kPa gage). Quantitative flow visualization data acquired by PSP sensor for this flow condition are shown in Fig. 11. The color scale on the PSP sensor images ranges from pure nitrogen (dark blue) to atmospheric conditions (dark red). A photographic bellows and a CCD camera were applied to create an image 4 × life size on the image plane. The dimensions

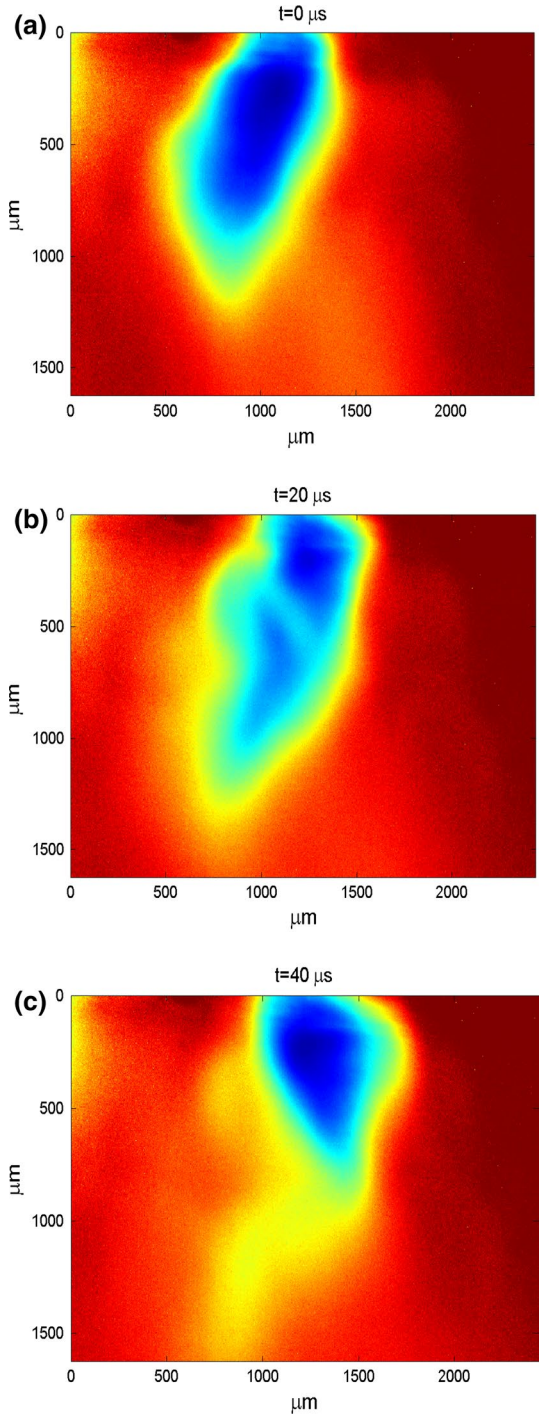

Fig. 11 Phase-averaged images through one period of the jet oscillation. Figure reprinted with permission from Prof. James Gregory. (Gregory et al. 2007)

on the axes of the images were calibrated by imaging a scale with 100 lines per inch and determining the imaging area of each pixel. Note that the entire image area covers a region measuring approximately 2,000 μm square, with each pixel representing an area measuring 3.2 μm square.

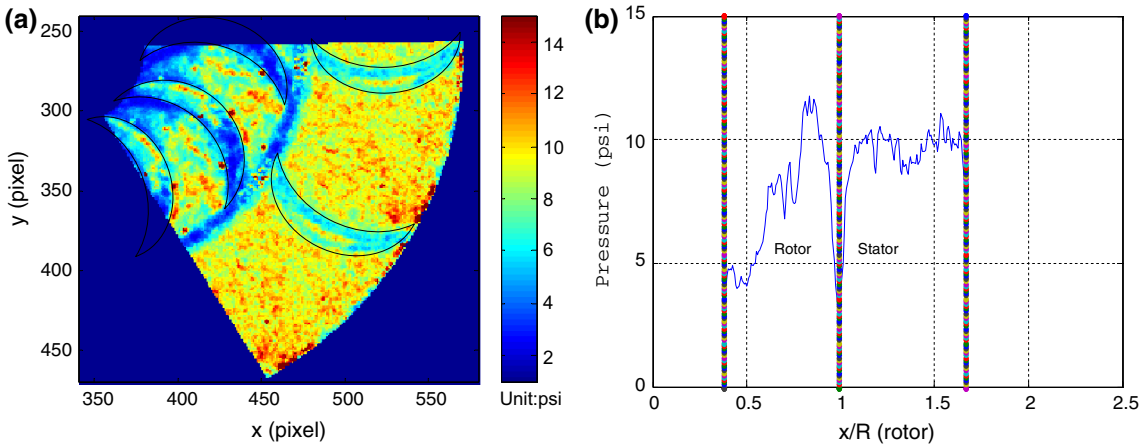

Fig. 12 **a** Phase-averaged pressure data inside a microturbine **b** pressure distribution from stator to rotor inside a microturbine. Figure adapted from Huang et al (2006) with permission of The American Society of Mechanical Engineers (Huang et al. 2006)

The data shown in Fig. 11 are phase-averaged through one period of the jet oscillation, with each image representing successive time delays from a fixed trigger. Each image is separated by 20 μs or approximately 19 % of the total cycle. These time steps were selected to represent approximately half of the oscillation period.

4.3.2 Pressure measurements in a microturbine

The microturbine is a microfluidic device that converts the fluid flow to work output, a component which has been utilized for constructing micro-engines. During the design and test of these devices, challenges such as vibration and massive heat generation inside the microturbine have been reported. Thus, a detailed investigation of flow field inside the microturbine device is a priority for solving these issues. The small size of PSP sensor as well as the fast response time (~10 μs) makes it a powerful technique for acquiring pressure data inside microturbine devices. The pressure distribution inside a microturbine device has been acquired with phase-averaged method between rotors and stators in Fig. 12. These pressure data were acquired at low rotation speed around thousands of rpm, which is restricted by unstable vibration from the rotor while rotating at higher speed. These preliminary results from microturbine measurement demonstrate the feasibility of applying PSP sensor in microscale unsteady flow measurement (Huang et al. 2006).

4.4 Oxygen detection in microfluidic devices

In addition to pressure measurement at microscale, PSP applications have also been extended to the measurements of oxygen concentration (Borisov and Klimant 2009; Sakaue et al. 2009). This kind of measurement uses the oxygen sensitivity of PSP to monitor the oxygen level in

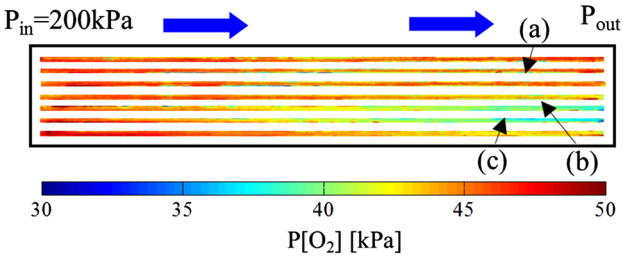

Fig. 13 Oxygen partial pressure distribution in a fuel cell visualized by PSP sensor. Figure adapted from Inagaki et al (2007) with permission of The American Society of Mechanical Engineers (Inagaki et al. 2007)

microfluidic channel in fuel cells (Inukai et al. 2008). The PSP technique has been used to understand the dynamic behavior of oxygen molecules and oxygen concentration distribution over electrode planes and inside diffused layers to improve the efficiency and sustainability of a fuel cell. It is particularly indispensable to know when, where, and how oxygen is consumed in the fuel cell for developing the design guide. Inagaki et al. (2007) applied the PSP sensor technique to the measurement of the oxygen partial pressure distribution in a fuel cell to improve power generation. The PSP sensor was composed of PtTFPP as the sensor probe, polystyrene with a low molecular weight (Mw = 100,000) as the binder, toluene, and a water-repellent agent. Figure 13 shows the oxygen partial pressure distribution in a fuel cell in the case of power generation test. In the test, air flows from left to right in the transparent separator while initial pressure of the inlet of the channels is 200 kPa (oxygen partial pressure is 42 kPa). The cell temperature is controlled at 323 K by putting a heater at the back of the cell. The result shows that the oxygen partial pressure decreases from the gas inlet to the outlet along the channels; however, the trend is different in each channel. The oxygen consumption along

the channel (c) is extremely rapid compared with that in the channel (a) where the oxygen consumption is slow. Similar application measuring oxygen concentration has also been carried out by Maruyama et al. (2012), Matsuda et al. (2011b). A luminescent sensor film is developed to study the dissolved oxygen (DO) in unsteady 2D flow field (periodic oscillatory flow), and the acquired results agree with that measure by fluorescein-seeded flow at frequency of 0.72 Hz. These studies demonstrate the feasibility of adapting PSP sensors for DO measurements.

5 Future aspects

The future development of PSP technique in microscale measurements will be focused on enhancing luminescence intensity, by exploring different luminophores or combining sensor molecules by copolymerization, and refining spatial resolution to sub-micrometer with fluorescence microscopes. Low luminescence signal in PSP measurements due to thin layer of PSP sensor results in poor signal-to-noise ratio and poses barrier for applying several calibration methods such as lifetime decay method, which has the potential of resolving temperature dependence and simultaneous temperature and pressure measurements. The spatial resolution from PSP measurement can be further improved with progressing microscopes and CCD technologies. CCD cameras with high pixel resolution can be easily found in the market with affordable price. However, a proper calibration using two-dimensional oxygen permeation assumption instead of one-dimensional is suggested for better translation of pressure profiles with sub-micrometer resolution. In addition, the development of new reaction principal using fluorescence resonance energy transfer for detecting pressure variation is one of the possible research aspects (Hamner 2008). Further applications of PSP measurement in free-molecular flow regime are also new interests of researchers; however, the consideration on molecular flux calculation from luminescence signal is required while presenting the experimental data.

Using PSP technique, detailed pressure profile with two-dimensional information can be acquired, and the information is helpful for analyzing asymmetrical flow field. Although this technique is limited to surface pressure measurement, it is capable of studying microflow field in most flow regimes. PSP measurements facilitate the investigation of micro gas flow in aggressive geometrical change such as constrictions or sharp bend, as well as the oxygen detection or gases mixing. In addition, the application of PSP measurements to study the gas dynamics of shockwave behaviors in microscale would draw great interests from researchers in the fields of microrockets and satellites.

6 Conclusions

The methodology and applications of PSP sensors at microscale have been presented and discussed in this review. The applications of PSP sensors on microscale measurements in different flow regimes include transition flow, supersonic flow, and unsteady flow. Results from these experiments performed in various microdevices and test conditions have been successfully acquired, and some results have been compared with theoretical or numerical data with good agreement. In general, PSP technique can provide detailed pressure information in flow field at microscale, and it is worthwhile to take the advantages of PSP technique and continue the studies as well as the applications in microfluidic research.

References

Agrawal A (2011) A comprehensive review on gas flow in microchannels international. J Micro Nano Scale Transp 2:1–40

Alexeenko AA, Gimelshein SF, Levin DA, Collins RJ (2000) Numerical modeling of axisymmetric and three-dimensional flows in MEMS nozzles. Paper presented at the 36th AIAA/ASME/SAE/ASEE joint propulsion conference and exhibit, Huntsville, AL

Beskok A (2001) Validation of a new velocity-slip model for separated gas microflows. Numer Heat Transf B Fund 40:451–471

Beskok A, Karniadakis GE, Trimmer W (1996) Rarefaction and compressibility effects in gas microflows. J Fluid Eng T ASME 118:448–456

Borisov SM, Klimant I (2009) Luminescent nanobeads for optical sensing and imaging of dissolved oxygen. Microchim Acta 164:7–15

Buoni M, Dietz D, Aslam K, Subramaniam VV (2001) Simulation of compressible gas flow in a micronozzle. Paper presented at the 35th AIAA thermophysics conference, Anahiem, CA

Chamarthy P, Garimella SV, Wereley ST (2010) Measurement of the temperature non-uniformity in a microchannel heat sink using microscale laser-induced fluorescence. Int J Heat Mass Transf 53:3275–3283. doi:10.1016/j.ijheatmasstransfer.2010.02.052

Chiang K-C, Wang Y-W, Chen Y-H, Wang H-Y, Huang C-Y (2013) The study of asymmetric flows in constricted microchannel with PSP technique. Paper presented at the tenth international conference on flow dynamics, Sendai, Japan

Crafton J, Lachendro N, Guille M, Sullivan JP (1999) Application of temperature and pressure sensitive paint to an obliquely impinging jet. Paper presented at the AIAA 37th aerospace sciences meeting and exhibit, Reno, NV

Crafton J, Fonov S, G. J, Fonov V, Goss L, Tyler C (2005) Simultaneous measurements of pressure and deformation on a UCAV in the SARL. Paper presented at the 43rd AIAA aerospace sciences meeting and exhibit, Reno, Nevada

Goss L, Jones G, Crafton J, Fonov S (2005) Temperature compensation for temporal (lifetime) pressure sensitive paint measurements. Paper presented at the 43rd AIAA aerospace sciences meeting and exhibit, Reno, Nevada

Gregory J, Sullivan J, Raghu S (2005) Visualization of jet mixing in a fluidic oscillator. J Vis 8:169–176

Gregory J, Sullivan J, Raghu S (2007) Characterization of the microfluidic oscillator. AIAA J 45:568–576. doi:10.2514/1.26127

Gregory JW, Sakaue H, Liu TS, Sullivan JP (2014) Fast pressure-sensitive paint for flow and acoustic diagnostics. Annu Rev Fluid Mech 46:303–330

Guo XH, Huang CY, Alexeenko A, Sullivan J (2008) Numerical and experimental study of gas flows in 2D and 3D microchannels. J Micromech Microeng 18:025034. doi:10.1088/0960-1317/18/2/025034

Hamner MP (2008) Developing new nano-materials for use as pressure-sensitive coatings. Meas Sci Technol 19:095021. doi:10.1088/0957-0233/19/9/095201

Ho CM, Tai YC (1996) Review: MEMS and its applications for flow control. J Fluid Eng T ASME 118:437–447

Ho C, Tai Y (1998) Micro-electro-mechanical-systems (MEMS) and fluid flows. Annu Rev Fluid Mech 30:579–612

Hong CP, Yamada T, Asako Y, Faghri M (2012) Experimental investigations of laminar, transitional and turbulent Gas flow in microchannels. Int J Heat Mass Transf 55:4397–4403

Huang C (2006) Molecular sensors for MEMS. Ph.D dissertation, Purdue Univerisity

Huang C, Gregory J, Sullivan J (2008) Pressure and temperature measurements of supersonic microjet impingement. Paper presented at the XXII international congress of theoretical and applied mechanics, Adelaide, Australia

Huang C, Sakaue H, Gregory J, Sullivan J (2002) Molecular sensors for MEMS. In: 40th Aerospace sciences meeting & exhibit

Huang CY, Lai CM (2012) Pressure measurements with molecule-based pressure sensors in straight and constricted PDMS microchannels. J Micromech Microeng 22:065021. doi:10.1088/0960-1317/22/6/065021

Huang C, Gregory J, Nagai H, Asai K, Sullivan J (2006) Molecular sensors in microturbine measurement. Paper presented at the ASME international mechanical engineering congress & exposition

Huang C, Gregory J, Sullivan J (2007a) Flow visualization and pressure measurement in micronozzles. J Vis 10:281–288

Huang C, Gregory J, Sullivan J (2007b) Microchannel pressure measurements using molecular sensors. J Microelectromech Syst 16:777–785. doi:10.1109/Jmems.2007.892914

Huang CY, Lai CM, Li JS (2012) Applications of pixel-by-pixel calibration method in microscale measurements with pressure-sensitive paint. J Microelectromech Syst 21:1090–1097. doi:10.1109/Jmems.2012.2203106

Inagaki S, Nagai H, Asai K (2007) Measurement of oxygen partial pressure distribution in a fuel cell using pressure-sensitive paint. In: Proceedings of 2007 ASME–JSME thermal engineering summer heat transfer conference, Vancouver, BC, Canada

Inukai J et al (2008) Direct visualization of oxygen distribution in operating fuel cells. Angew Chem Int Edit 47:2792–2795

Ivanov MS, Markelov GN, Ketsdever AD, Wadsworth DC (1999) Numerical study of cold gas micronozzle flows. Paper presented at the 37th aerospace sciences meeting & exhibit, Reno, NV

Jie D, Diao X, Cheong KB, Yong LK (2000) Navier–Stokes simulations of gas flow in micro devices. J Micromech Microeng 10:372–379

Karniadakis G, Beskok A (2002) Micro flows: fundamentals and simulation. Springer, New York

King C, Walsh E, Grimes R (2007) PIV measurements of flow within plugs in a microchannel. Microfluid Nanofluidics 3:463–472

Liu T, Sullivan JP (2004) Pressure and temperature sensitive paints. Springer, Berlin

Maruyama H, Matsuda Y, Uozumi N, Nanatani K, Arai F (2012) Measurement of photosynthesis using single synecocystis SP. 6803 on a micro chamber with gas barrier wall. Paper presented at the 16th international conference on miniaturized systems for chemistry and life sciences, Okinawa, Japan

Matsuda Y, Mori H, Niimi T, Uenishi H, Hirako M (2007) Development of pressure sensitive molecular film applicable to pressure measurement for high Knudsen number flows. Exp Fluids 42:543–550. doi:10.1007/s00348-007-0259-5

Matsuda Y, Mori H, Sakazaki Y, Uchida T, Suzuki S, Yamaguchi H, Niimi T (2009a) Development of pressure sensitive molecular film as a measurement technique for micro-flows rarefied gas. Dynamics 1084:527–532

Matsuda Y, Mori H, Sakazaki Y, Uchida T, Suzuki S, Yamaguchi H, Niimi T (2009b) Extension and characterization of pressure-sensitive molecular film. Exp Fluids 47:1025–1032. doi:10.1007/s00348-009-0694-6

Matsuda Y, Misaki R, Yamaguchi H, Niimi T (2011a) Pressure-sensitive channel chip for visualization measurement of micro gas flows. Microfluid Nanofluidics 11:507–510. doi:10.1007/s10404-011-0825-2

Matsuda Y, Nagashima F, Yamaguchi H, Egami Y, Niimi T (2011b) Unsteady 2D measurement of dissolved oxygen distribution using luminescent sensor film. Sens Actuat B-Chem 160:1464–1467

Matsuda Y, Uchida T, Suzuki S, Misaki R, Yamaguchi H, Niimi T (2011c) Pressure-sensitive molecular film for investigation of micro gas flows. Microfluid Nanofluidics 10:165–171. doi:10.1007/s10404-010-0664-6

Matsuda Y, Yamaguchi H, Egami Y, Niimi T (2012) A discussion of spatial resolution of pressure-sensitive paint. Trans Jpn Soc Mech Eng Ser B 78:1260–1266

Meinhart CD, Gray HB, Wereley ST (1999a) PIV measurements of high-speed flows in silicon-micromachined nozzles. Paper presented at the 30th AIAA fluid dynamics conference, Norfolk, VA

Meinhart CD, Wereley ST, Santiago JG (1999b) PIV measurements of a microchannel flow. Exp Fluids 27:414–419

Mitsuo K, Asai K, Takahashi A, Mizushima H (2006) Advanced lifetime PSP imaging system for pressure and temperature field measurement. Meas Sci Technol 17:1282–1291

Mori H, Niimi T, Hirako M, Uenishi H (2005) Molecular number flux detection using oxygen sensitive luminophore. Phys Fluids 17:100610. doi:10.1063/1.1921927

Morini GL, Yang YH, Chalabi H, Lorenzini M (2011) A critical review of the measurement techniques for the analysis of gas microflows through microchannels. Exp Therm Fluid Sci 35:849–865

Mosharov VE, Fonov SD, Radchenko VN (1997) Luminescent pressure sensors in aerodynamic experiments. Central Aerohydrodynamic Institute, Moscow

Nagai H, Naraoka R, Sawada K, Asai K (2008) Pressure-sensitive paint measurement of pressure distribution in a supersonic micronozzle. AIAA J 46:215–222. doi:10.2514/1.28371

Nguyen N-T, Wereley ST (2002) Fundamentals and applications of microfluidics. Microelectromechanical systems series. Artech House, Boston

Osafune T, Kurotaki T, Asai K (2004) Application of molecular sensors to micro objects in supersonic flow. Paper presented at the 42nd AIAA aerospace sciences meeting and exhibit, Reno, Nevada

Peng D, Gregory J, Crafton J, Fonov S (2010) Development of a two layer dual-luminophore pressure sensitive paint for unsteady pressure measurements. Paper presented at the 27th AIAA aerodynamic measurement technology and ground testing conference, Chicago, IL

Pong K, Ho C, Liu J, Tai Y (1994) Non-linear pressure distribution in uniform micro channels. In: ASME winter annual meeting

Roy S, Raju R, Chuang HF, Cruden BA, Meyyappan M (2003) Modeling gas flow through microchannels and nanopores. J Appl Phys 93:4870–4879

Sakamura Y, Suzuki T, Kawabata S (2014) Development and characterization of a pressure-sensitive luminescent thin coating based on Pt(II)-Porphyrin self assembled monolayers. Paper presented

at the 16th international symposium on flow visualization, Okinawa, Japan

Sakaue H, Ozaki T, Ishikawa H (2009) Global oxygen detection in water using luminescent probe on anodized aluminum. Sens Basel 9:4151–4163

Song WZ, Psaltis D (2011) Optofluidic membrane interferometer: an imaging method for measuring microfluidic pressure and flow rate simultaneously on a chip. Biomicrofluidics 5:44110–4411011. doi:10.1063/1.3664693

Tang GH, Li Z, He YL, Tao WQ (2007) Experimental study of compressibility, roughness and rarefaction influences on microchannel flow. Int J Heat Mass Transf 50:2282–2295

Wereley ST, Jang J (2004) Pressure distributions of gaseous slip flow in straight and uniform rectangular microchannels. Microfluid Nanofluidics 1:41–51. doi:10.1007/s10404-004-0005-8

Yamaguchi H, Matsuda Y, Mori H, Niimi T (2009) Discussion on measurement mechanism of pressure-sensitive paints. Sens Actuators B Chem 142:224–229. doi:10.1016/j.snb.2009.07.022

Zare-Behtash H, Gongora-Orozco N, Kontis K, Holder SJ (2009) Application of novel pressure-sensitive paint formulations for the surface flow mapping of high-speed jets. Exp Therm Fluid Sci 33:852–864

Zohar Y, Lee SYK, Lee WY, Jiang LN, Tong P (2002) Subsonic gas flow in a straight and uniform microchannel. J Fluid Mech 472:125–151. doi:10.1017/S0022112002002203